Low Temperature Physics/Fizika Nizkikh Temperatur, 2012, v. 38, No. 1, pp. 20–27

Liquid ^{3}He–^{4}He mixture phase diagram in restricted geometry

I.A. Degtiarov and S.S. Sokolov

B. Verkin Institute for Low Temperature Physics and Engineering of the National Academy of Sciences of Ukraine
47 Lenin Ave., Kharkov 61103, Ukraine
E-mail: degtiarov.igor@gmail.com

Received June 24, 2011

The influence of van der Waals forces on the decay of liquid solutions of helium isotopes is studied theoretically and the conditions for the phase co-existence in a confined geometry are investigated. As the models to account the influence of van der Waals forces on the helium isotope solution the gap between two parallel planes and the cylindrical channel are considered. For each of the models we calculated the concentration profile inside the channel depending on the van der Waals constant, the initial solution concentration and the size of the channel. The phase diagrams of liquid solutions are constructed. The obtained liquid mixture phase diagrams are compared with the "bulk" phase diagram. A rather good agreement between theoretical and experimental phase diagrams is obtained for liquid helium mixture in aerogel.

PACS: **67.10.–j** Quantum fluids: general properties;
67.60.–g Mixtures of ^{3}He and ^{4}He;
67.60.gj Restricted geometries.

Keywords: helium isotopes, liquid solutions, phase diagram of liquid solutions ^{3}He–^{4}He.

Introduction

The phase diagram of liquid solutions ^{3}He–^{4}He [1] and, in particular, the finite solubility of ^{3}He in a phase riched in ^{4}He which arises under stratification of homogeneous solution (the corresponding concentration $x \simeq 6.7\%$ at $T = 0$), lead to very interesting thermodynamic and kinetic properties of such solutions. The superfluid solutions are paid the special attention. Superfluid liquid mixture of ^{3}He–^{4}He can penetrate into the small pores and channels, and there is a unique opportunity to study the thermodynamic and other characteristics of solutions of quantum liquids ^{3}He and ^{4}He in a "narrow" geometry. Such studies are very popular in recent decades, particularly by the example of aerogels, which is a highly porous medium from a glassy material that is filled with helium [2–7]. Another example of a porous medium, where such research is provided, is vycor [8,9], glassy material, much more dense than aerogel, in which the cavity filled with helium, form a system of regular channels located far enough from each other. The characteristic channel size in vycor varies in 20–100 Å. It was established experimentally that the phase diagram of a solution ^{3}He–^{4}He in a porous substance is different of that in bulk case (see Fig. 1). It turned out that the phase diagram depends strongly on the porosity of the material, which is filled by a solution. One should consider separately aerogels with a porosity of $\gtrsim$ 95% and $\lesssim$ 95% (according to [7] at a porosity $\sim$95% deviation of the phase diagram of bulk case practi-

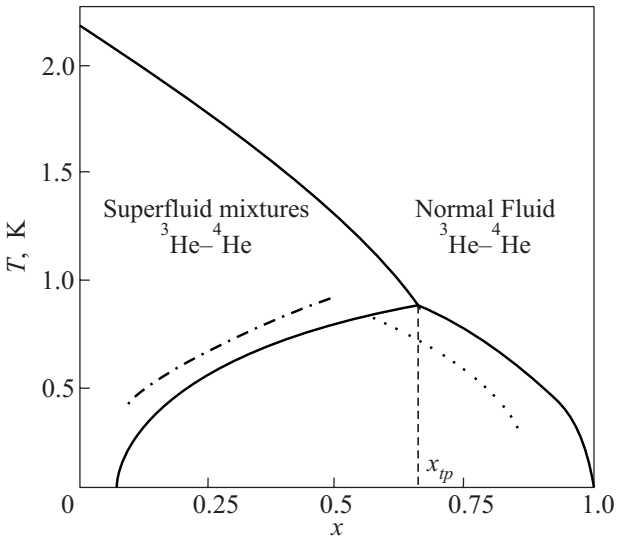

Fig. 1. Phase $x-T$ diagram of liquid solutions ^{3}He–^{4}He. Solid line — bulk phase diagram. The dotted curve is qualitatively shown deviation from the bulk phase diagram in aerogel with a porosity of more than 95% [2,3], dash-dotted line is a deviation of the phase diagram from the bulk case, observed at a porosity of less than 95% [4–6].

cally was not observed.) Note that, as evidenced by acoustic studies [10], carried out for pure ^{4}He, the structure of aerogels is different in these ranges of porosity, as it follows from the change in temperature dependence of the sound velocity. If the aerogel is dense (porosity less than 95%), such a dependence corresponds to a velocity of fourth sound in a narrow capillary, whereas to a velocity of first sound in a bulk liquid in the opposite limit of a more rarefied medium. One can guess that a dense aerogels is similar to vycor being an environment that can be approximated by a set of loosely coupled individual channels in a dense glass whereas the rarefied aerogel is almost hollow medium filled with helium and has interwoven glass fiber located relatively far from each other. The difference in the structure of aerogels affects the form of the phase diagram of liquid helium isotopes solution.

If the porosity of aerogels is $\gtrsim 95\,\%$ the deviation of the phase diagram from that in bulk liquid is observed in right branch with $x_{tp} < x < 1$ [2,3] (see Fig. 1). This deviation of the phase diagram is qualitatively explained in [11], where the phase diagram was studied by the Monte Carlo, taking into account changes in the chemical potential near randomly administered impurity molecules SiO_2. For the porosity of aerogels $\lesssim 95\,\%$, the whole phase diagram of liquid solutions "shifted" [4–6], this effect is associated with a change in concentration of the solution by forming a solid layer of pure ^{4}He on the glass surface. However the detailed analysis of this fact accounting for a solid monolayer of ^{4}He on the wall, demonstrated that the deviation of the phase diagram is observed only on the left branch (with $0 < x < x_{tp}$) of the phase diagram describing the stratification of solutions (see Fig. 1). The same idea was proposed to explain qualitatively the deviation of observed phase diagram from that in bulk observed for liquid solutions of helium isotopes in vycor [8]. However, quantitative calculation of this effect, unfortunately, was not presented.

Thus the question with associated features of the thermodynamic properties of solutions of helium isotopes placed in the porous structure remains valid.

The aim of present paper is to study the conditions of phase co-existence of liquid solutions of helium isotopes in a confined geometry, depending on the characteristic size of the channel filled with liquid, as well as for various substances that form a porous medium. We believe that, in the narrow geometry, the determining influence on the condition of co-existence have the van der Waals forces, because of what one should investigate the conditions of thermodynamic equilibrium in a field of such forces. We study two geometric models of the porous medium and investigate the effect of the van der Waals constant on the thermodynamic characteristics of the solution ^{3}He–^{4}He. The results obtained allow to construct the phase diagrams being in qualitative agreement with those observed experimentally.

2. The influence of van der Waals forces on liquid solutions of ^{3}He–^{4}He

We model the porous structure filled with liquid solution of the helium isotopes as a closed surface formed by strands of SiO_2, which form channels and pores. Liquid solutions of helium isotopes fill the void. The key point of the analysis is the chemical potential of the liquid. Here we restrict ourselves to the approach of ideal solutions taking in mind mainly qualitative consideration of the problem and write the chemical potentials of each component of a "bulk" solution as [12]:

$$\mu_j = \mu_{0j} + T \ln e \frac{N_j}{N}; \tag{1}$$

index $j =$ 3 or 4 stands for ^{3}He and ^{4}He, respectively; μ_{0j} is uniform chemical potential of pure helium isotopes; N_j is partial number of atoms of each isotope and N the total number of atoms. Concentration of ^{3}He in the solution is $x = N_3 / N$. To account for the influence of the channel walls, we should supplement the (1) by additional term associated with a potential U of van der Waals forces acting between helium and the walls of the channel, which leads to the following conditions [12,13]:

$$\begin{cases} \mu_3(x,T,P) + U = \text{const}, \\ \mu_4(x,T,P) + U = \text{const}. \end{cases} \tag{2}$$

Taking into account that $d\mu_{0j} = v_j dP$, where v_j are atomic volumes and P is the pressure of (2) we arrive to the following equations:

$$\begin{cases} v_3 dP + \dfrac{T}{x} dx + dU(\xi) = 0, \\ v_4 dP + \dfrac{T}{1-x} d(1-x) + dU(\xi) = 0; \end{cases}$$

where ξ being the direction normal to the channel walls. We multiply the first equation by $(1-x)$, and then second by x, and then add them. Also we subtract one equation from other and finally obtain a system of equations defining the conditions of thermodynamic equilibrium:

$$\begin{cases} v dP = -dU(\xi), \\ d \ln\left(\dfrac{x}{1-x}\right) = \dfrac{\Delta v}{T} dP. \end{cases} \tag{3}$$

where $\Delta v = v_3 - v_4$. From the first equation we find the differential pressure

$$dP = -\frac{dU(\xi)}{v} = -\frac{dU(\xi)}{x v_3 + (1-x) v_4}. \tag{4}$$

Substituting this expression into the second equation, we obtain:

$$d \ln\left(\frac{x}{1-x}\right) = -\frac{\Delta v}{T} \frac{dU(\xi)}{x v_3 + (1-x) v_4}. \tag{5}$$

Rewrite (5) in the form

$$\left[\frac{v_3}{1-x}+\frac{v_4}{x}\right]dx=\frac{\Delta v}{T}dU(\xi), \tag{6}$$

and integrating (6), we obtain, for $x(\xi)$:

$$\frac{Cx(\xi)}{\left[1-x(\xi)\right]^{v_3/v_4}}=\exp\left[\frac{\Delta v}{v_4 T}U(\xi)\right]. \tag{7}$$

For further consideration we will need to use the explicit form of the potential of van der Waals force acting between the walls of the channel and the helium isotopes, and to choose the geometry of the channel filled with fluid. The real geometry of aerogel and vycor is too complicated and irregular making intractable the description of van der Waals forces in it. For this reason we consider, as "limiting" geometries, two models:

— model of plane channel, bounded on two sides by two parallel planes;

— model of a hollow cylinder.

As we will see the results for these two geometries differ only qualitatively guessing that the results for real geometry would be close to those of simple geometries we consider.

2.1. The model of a narrow plane-parallel channel

The potential of the van der Waals forces for the plane is well known, it can be written as:

$$U(\xi)=U(z)=-\frac{a}{z^3}, \tag{8}$$

where a being the van der Waals constant of substance of the channel walls, the axis z is supposed to be perpendicular to the plane which forms the channel.

If we have a channel, bounded on two sides, one should take into account the influence of van der Waals forces from each of the planes. Then the interaction potential $U(z)$ becomes

$$U(z)=-\frac{a}{z^3}-\frac{a}{(D-z)^3}, \tag{9}$$

where D is the distance between the planes forming the channel.

To calculate $x(z)$ using (7) one has to determine the constant of integration. We determine the value of C from the condition that at $z = D/2$

$$C=\frac{\left[1-x(D/2)\right]^{v_3/v_4}}{x(D/2)}\exp\left[\frac{\Delta v}{v_4 T}U(D/2)\right], \tag{10}$$

that is, to determine the integration constants C we need to find the value of the concentration $x(D/2)$ in the center of channel. To set the value of $x(D/2)$, we use an additional condition which is imposed on the function $x(z)$. The solution in a narrow channel is characterized by a redistribution of concentrations. The concentration profile is shown schematically in Fig. 2,*a*. The initial "bulk" concentration of the solution corresponds to x_0, shown in Fig. 2. The Maxwell rule (law of conservation of matter) should be satisfied, according to which areas of S_1 and S_2 must be equal (Fig. 2,*b*). From the Figure one, can see

$$S_1=(z_0-d_s)x_0-\int_{d_s}^{z_0}x(z)\,dz;$$

$$S_2=\int_{z_0}^{D/2}x(z)\,dz-(D/2-z_0)x_0,$$

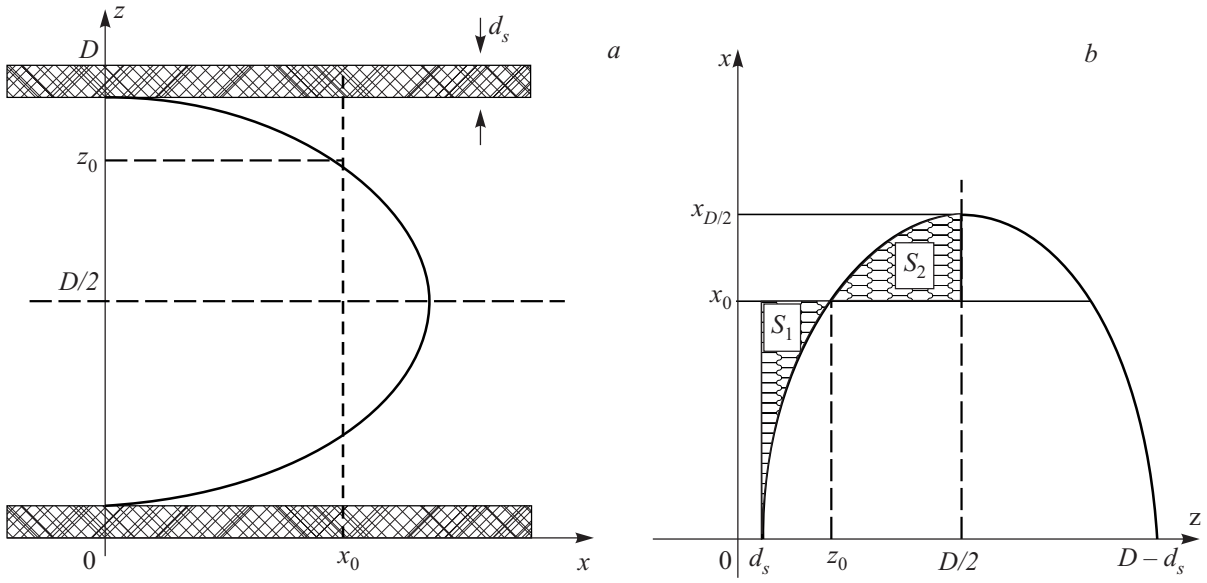

Fig. 2. Concentration profile in the two-dimensional narrow channel. d_s — the thickness of the solid ^{4}He at the channel walls; D — the channel width; x_0 — the initial concentration of solution (*a*); the law of conservation of matter, which requires that the space S_1 and S_2 are equal to each other (*b*).

where $d_s \simeq 5$ Å is a width of the solid inert layer of pure ^{4}He [13], z_0 is determined by condition $x(z_0) = x_0$. To estimate the initial concentration of the mixture we take into account the solid layer of pure ^{4}He, that is formed on the walls of the channels. In this case the concentration inside the channel is greater than in bulk. The initial concentration inside channels with $D = 20$ Å increases in 2 times in comparison with bulk case, in channels $D = 100$ Å increases 1.1 times, and in channels 500 Å increases only 1.02 times. Under further increase of channels width the initial concentration does not change practically.

Equating the areas S_1 and S_2, we obtain the following conditions which $x(z)$ must satisfy:

$$\int_{d_s}^{D/2} x(z)\, dz = (D/2 - d_s)x_0; \quad x_0 < x_{D/2} < 1. \qquad (11)$$

Solving, in a self-consistent way, Eqs. (7) and (11) and taking into account (10), we can determine simultaneously the concentration profile of $x(z)$ and the value of $x(D/2)$, set C in (7). To realize such a scenario, we established an algorithm of numerical calculation, which allows to find $x(z)$ depending on the van der Waals constant and the channel width D. It should be noted that when the width of the channel is small enough, due to the action of van der Waals forces, the entire channel is overgrown with a solid ^{4}He and one cannot speak on a liquid solution in the channel. Thus, there is a natural limiting value of the width of the channel $D \gtrsim 10$ Å, for which our analysis remains valid.

Concentration profiles in the narrow channels for different a are shown in Fig. 3, and, depending on D for some x_0 in Fig. 4.

The Figure demonstrates that the stronger interaction of the solution with the channel walls, the greater the concentration varies with coordinate z. For narrow channels (Fig. 4,*a*) the concentration in the center can highly exceed

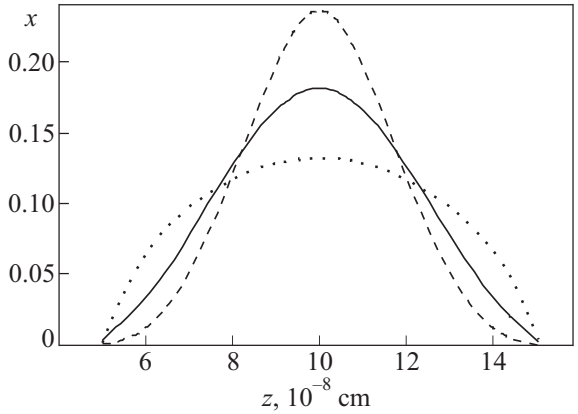

Fig. 3. Concentration profile of a narrow parallel channel for a solution of ^{3}He in the ^{4}He with an initial concentration of $x_0 = 0.1$. Van der Waals constants are taken for neon — dotted line, glass — solid line, metal — dashed line [14]. The width of the channel is $D = 20$ Å.

the initial concentration of solution. For example, in the channels of a width $D \sim 20$ Å the initial concentration is exceeded about twice for not very large x_0. In wide channels (Fig. 4,*b*), the essential difference from the bulk concentration can be observed only near the walls, in the channel center the solution concentration is almost exactly the same as the bulk concentration of the solution.

It should be emphasized that the channel center concentration is always above the initial concentration corresponding to the bulk case. In this connection the question arises how can change the phase diagram of the solution, placed in a narrow channel. Using the calculated concentration profile, we estimate the change in the phase diagram for different values of the width of the channels in the glass medium. As the criterion for choosing the solution concentration at which the stratification starts in a narrow channel, we took the value of concentration at the center of the channel, which is equal to the concentration of the stratification in a "bulk" solution where one disregards

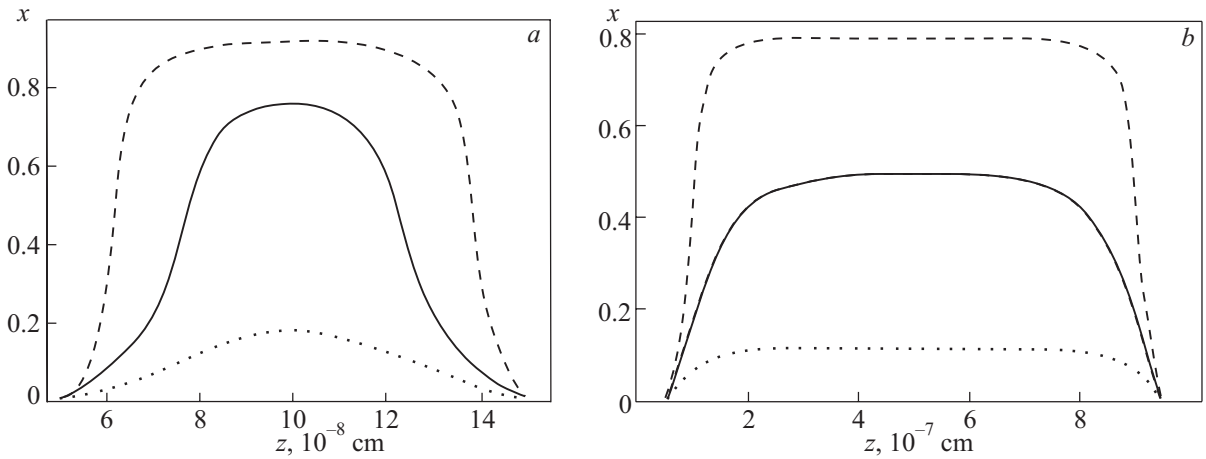

Fig. 4. Concentration profile of liquid solutions of helium isotopes across the channel width and for the some initial concentration of the solution. The width of the channel $D = 20$ Å (*a*) and 100 Å (*b*). The initial concentration of x_0 is equal to 0.1 — dotted line, 0.45 — solid line, and 0.8 — dashed line. The substance of the walls — glass.

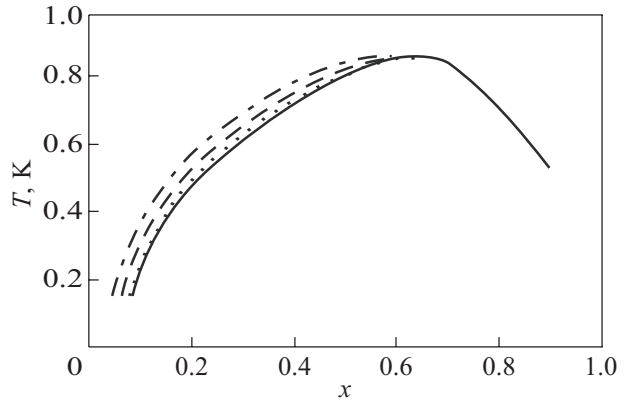

Fig. 5. Phase diagrams of solutions of ^{3}He–^{4}He for the bulk case — the solid curve and for narrow channel of width 50 Å — dot-dashed curve, 100 Å — dashed curve, 500 Å — dotted curve.

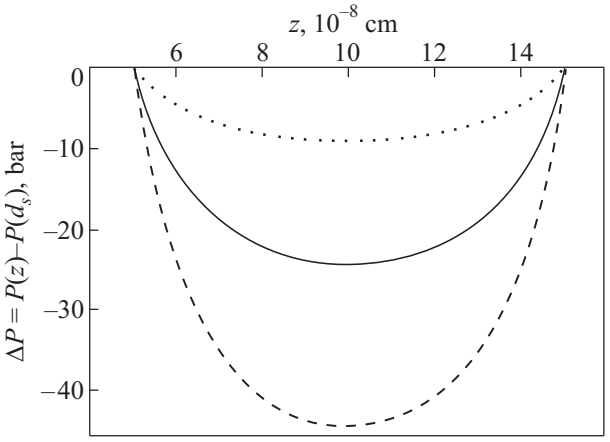

Fig. 6. Viewing excess pressure in the narrow gap between two plane-parallel planes for different coupling constants of van der Waals forces: the dotted line — neon, solid line — glass; dashed line — metal (constant Van der Waals forces of [14]). The width of the channel is $D = 20$ Å.

the influence of van der Waals forces, x_s^{vol}, that is, we took $x_{D/2} = x_s^{\text{vol}}$ for a given temperature T. Figure 5 shows the phase diagram for the bulk case and for the solution placed in a narrow plane-parallel channel for the different channel widths. It should be noted that the distribution of solution concentration in the channel will make changes only in the left branch of the phase diagram of stratification, when the bulk stratification concentration will be achieved in the center of channel. In the right branch of the phase diagram, such a distribution always leads to the fact that at a given temperature inside the channel, the stratification concentration is always achieved. Probably, for this reason only normal–superfluid transition was observed in the right branch of phase diagram whereas the phase transition of stratification was not observed. As can be seen from Fig. 5, the narrower is the channel and stronger interaction with the walls of the solution, the greater is the deviation of the phase diagram of the bulk case. With increasing D the deviation decreases and at $D \simeq 1000$ Å the influence of the walls on the phase diagram becomes negligible.

The applied method also allows, knowing the concentration distribution in a narrow channel and integrating the Eq. (4), find the pressure distribution in the channel:

$$\Delta P = P(z) - P(d_s) = -\frac{1}{v_4}\int_{d_s}^{z} \frac{\dfrac{dU(z)}{dz}}{\left[1+\dfrac{\Delta v}{v_4}x(z)\right]}\,dz\,. \quad (12)$$

An example of numerical calculation of the pressure profile is shown in Fig. 6.

2.2. The model of a narrow hollow cylinder

To describe the concentration distribution in a model of a narrow cylinder, we still use the Eq. (7), where the coordinate ξ is now the radial variable r. The main problem now is to modify the interaction potential of the van der Waals forces, compared with the planar case. We use the method previously applied in a theoretical consideration of collective hydrodynamic oscillations of stratified solution in cylindrical geometry [15]. The potential interaction between the liquid and solid substrate can be written in the gas approximation in the form:

$$U(\mathbf{r}) = -b_{\text{He–sol}} n_{\text{sol}} \int d\mathbf{r}' \int dz' \frac{1}{(|\,\mathbf{r}-\mathbf{r}'\,|^2 + |\,z-z'\,|^2)^3}, \quad (13)$$

where z is directed along the axis of the cylinder, and $b_{\text{He–sol}}$ is the interaction constant between helium atoms and the particles of wall matter, n_{sol} is the volume concentration of these particles. The expression (13) is written neglecting the interaction of helium atoms with each other compared to the interaction with the substance of the walls, which is true for most substances (except for solidified inert gases and hydrogen). In the case of plane geometry, gas approximation leads to the expression (8), if one makes the change $a \simeq \pi/6\, b_{\text{He–sol}} n_{\text{sol}}$. To obtain the dependence of $U(r)$ from a we have made the similar change in Eq. (13), which, after integration over z' and ϕ' is reduced to:

$$U(r,\phi) = -6a\int_R^\infty r'dr' \frac{\left[4(r^2+r'^2)E(m) - (r-r')^2 K(m)\right]}{(r-r')^4 (r+r')^3}, \quad (14)$$

where R being the channel radius, $E(m)$ and $K(m)$ are the complete elliptic integrals, the argument of which is equal to $m = 4rr'/(r+r')^2$.

Unfortunately, the integration over r' in the expression (14) cannot be done analytically. However, these integrals can be computed using numerical methods.

Substituting the Eq. (14) for the potential of van der Waals forces in the Eq. (7) we find the integration constant C in the center of a cylindrical channel, similarly to the

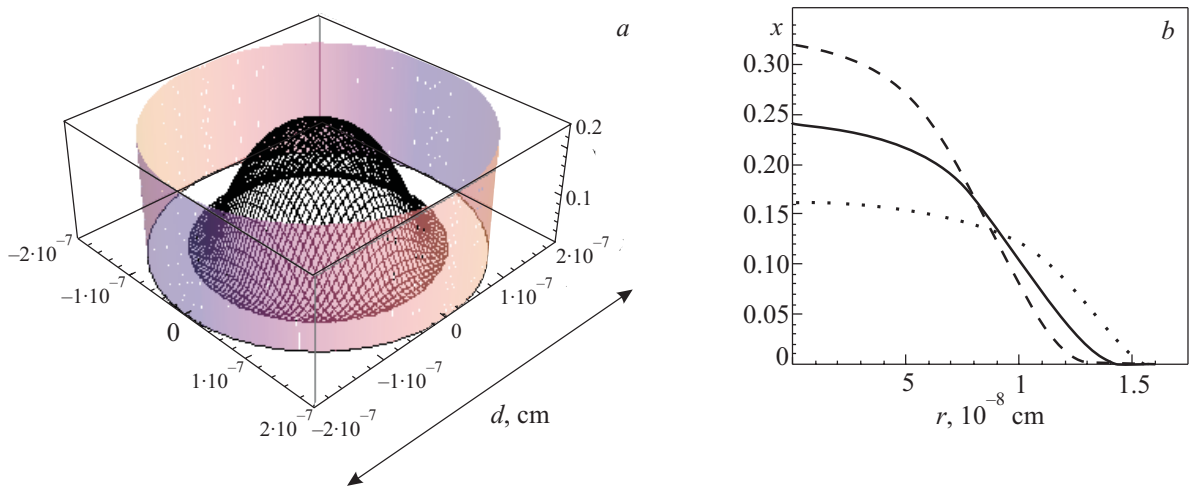

Fig. 7. Profiles of the concentrations of ^{3}He in solution ^{3}He–^{4}He in a narrow hollow cylinder, the substance of the walls — glass. The initial concentration of the solution $x_0 = 0.2$, the radius of the cylinder $R = 20$ Å (*a*); solution concentration $x_0 = 0.1$, with a radius of the cylinder $R = 20$ Å for the three constants of the van der Waals [14]: dotted line — neon, solid curve — glass, dashed curve — metal (*b*).

Eq. (10) (now $\xi = r$). Continuing to follow the above scheme for plane-parallel channel, we write the condition on the concentration of $x(r)$ inside the hollow cylinder of radius R:

$$\int_0^{R-d_s} rx(r)dr = \frac{(R-d_s)^2}{2}x_0; \quad x_0 < x_{\text{centre}} < 1. \quad (15)$$

As in the case of a plane geometry, we solve self-consistently (7) and (15), which makes it possible to construct the concentration profile in a narrow hollow cylinder depending on the parameters a, R and x_0. As noted above, the initial concentration within the channel is higher than the concentration in the bulk liquid because of the solid layer of ^{4}He, on the channel walls. So, for a cylindrical channel in the glass with a radius $R = 20$ Å the initial concentration in the channel increases by 2.4 times compared to the bulk concentration of the solution and for the channel radius $R = 500$ Å only 1.04 times. With further increase of the channel width, initial concentration remains practically unchanged.

The results of the calculation of the concentration profile in the cylindrical channel are presented in Fig. 7.

To construct the phase diagram of liquid solutions of helium isotopes in a hollow narrow cylinder we act similarly to the case of plane channel, which was reviewed in the previous section. The constructed phase diagram is shown in Fig. 8. As was expected, the narrower the channel, the stronger is the effect of helium interaction with the walls and the greater is the deviation of the phase diagram of the bulk case. It should be noted that the same characteristic width of the channel, in the case of the cylinder phase diagram, is different from the bulk case much stronger than in the case of a plane channel. As can be seen from Fig. 8, when the radius of the cylinder channel is about $R = 500$ Å one observes the deviation of the phase diagram from the bulk case, for $R = 100$ Å, and $R = 50$ Å deviation of the phase diagram becomes large enough, under a further decrease in the size of the cylinder, phase diagram of solutions of helium isotopes significantly shifted to the left. Thus, if we assume a porous substance cavity of cylindrical shape, then the radii $R \lesssim 500$ Å must show the shift to the left of the phase diagram. At smaller sizes of these cavities deviation of the phase diagram will become even more pronounced.

2.3. Comparison with experimental data

To compare the results of calculations with experimental data, we took data on the phase diagram of liquid solutions of helium isotopes in aerogel with porosity < 95% [4–6]. Recall that the deviation of the phase diagram in porous materials on the phase diagrams of solutions in the bulk case, is due to two facts. The first is the formation of a

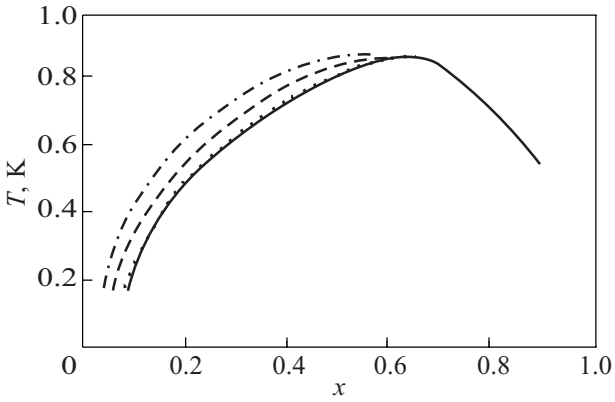

Fig. 8. Phase diagram in the "bulk" (solid line); in a hollow cylinder ($R = 500$ Å — dotted line, $R = 100$ Å — dashed line, $R = 50$ Å — dot-dashed curve. The substance of the walls — glass.

solid layer of ^{4}He at the surface of the channels, the second is the change of the concentration profile in the channels due to the influence of van der Waals forces acting on solution from the substrate. Accounting for changes in concentration due to formation of a solid layer implemented in the papers [4,5] for aerogels of porosity 85% and 87%, the experimental result on the deviation of the phase diagram of the bulk case in these works is almost identical. Therefore, we make a comparison with the results of [5]. Comparing the deviation of the phase diagram of solutions ^{3}He–^{4}He caused by the influence of van der Waals in aerogel, we can estimate the channel size that meets the experimental observation of a deviation, for both considered geometries (Fig. 9) even though our geometrical models are oversimplified and cannot pretend to describe the real aerogel.

We found that the calculated curves adjust the experimental data, in a plane model, for the width of the channel $D = 50$ Å and, for cylindric channel model for a channel radius $R = 100$ Å. The calculated phase diagrams are very close and are indistinguishable in the Fig. 9. That is why we restrict our estimates to a cylindrical channel. As is seen the models applied in our calculation adjust the experimental data reasonably well. At the same time, the most plausible, in the case of aerogels, is the result for a cylindrical channel with a pore diameter of 200 Å. Plane-parallel model assumes a pore size of about 50 Å. Note that similar dimensions of the channels in a porous substance are specific for vycor where the porosity is usually less than 30%.

3. Conclusions

The paper analyzes the thermodynamic properties of liquid mixtures of helium isotopes in the narrow geometry. The influence of van der Waals forces on the properties of the solution is considered and we show that the "offset" of phase diagram observed in experiments on liquid mixtures in aerogels and vycor may be due to the placement of fluid in the narrow geometry and the influence of wall material on a solution. The paper discusses two models: a narrow plane-parallel channel and the channel of cylindrical shape. We have shown that in the case of narrow channels coordinate-dependent concentration profile of ^{3}He arises, which has a minimum value at the channel wall and reaches a maximum at its center. Although qualitatively, in both models, the effect of van der Waals forces on the thermodynamic properties of liquid solutions is the same, the geometry of the channel affects the effect quantitatively. The deviation of the phase diagram from that in bulk is well seen for the channel size 20–100 Å, and if the size of the channel is $\gtrsim 500$ Å, the effect is practically absent. In the case of a cylindrical channel deviation of the phase diagram from the bulk is stronger than that for plane channel.

The obtained results well describe the experimentally observed data on the phase diagram of solutions ^{3}He–^{4}He in aerogel. At the same time, the model of a hollow cylindrical channel seems more plausible to describe the porous material than the model of plane-parallel channel, because the model of a cylindrical hollow channel gives a more realistic pore size. For a detailed agreement with the experimental data one requires more information about the geometrical structure of pores in the sample and calculations corresponding to this geometry, taking also into account the possible mutual influence of closely spaced channels.

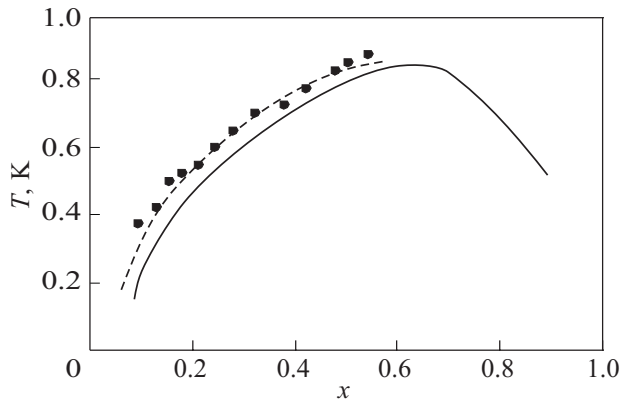

Fig. 9. Comparison of the experimental data on the deviation of the phase diagram of the bulk case with the calculation. The solid line shows the phase diagram for the bulk case. Filled circles — experimental points [5]; dashed line — a model of a cylindrical channel of radius $R = 100$ Å.

Acknowledgments

The work is partially supported by STCU program through the project 5211.

The authors are greatly indebted to E.Ya. Rudavskii, V.K. Chagovets, and A.A. Zadorozhko for useful discussions.

1. B.N. Esel'son, V.N. Grigor'ev, V.G. Ivantsov, E.Ya. Rudavskii, D.G. Sanikidze, and I.A. Serbin, *Solutions of Quantum Liquids* ^{3}He–^{4}He, Moscow, Nauka (1973).
2. J. Ma, S.B. Kim, L.W. Hrubeshand, and M.H.W Chan, *J. Low Temp. Phys.* **93**, 945 (1993).
3. N. Mulders, J. Ma, S.B. Kim, J. Yoon, and M.H.W. Chan, *J. Low Temp. Phys.* **101**, 95 (1995).
4. M. Paetkau and J.R. Beamish, *Czech. J. Phys.* **46**, 153 (1996).
5. M. Paetkau and J.R. Beamish, *Phys. Rev. Lett.* **80**, 5591 (1998).
6. J. Yoon, N. Mulders, L.W. Hrubeshand, and M.H.W. Chan, *Czech. J. Phys*. **46**, 157 (1996).
7. J. Yoon, N. Mulders, and M.H.W. Chan, *J. Low Temp. Phys.* **110**, 585 (1998).
8. T. Hohenberger, R. Konig, and F. Pobell, *J. Low Temp. Phys.* **110**, 579 (1998).

9. J.R. Beamish, A. Hikata, L. Tell, and C. Elbaum, *Phys. Rev. Lett*. **7**, 425 (1983).
10. A.A. Zadorozhko, V.K. Chagovets, E.Ya. Rudavskii, G.A. Sheshin, Sh.E. Kekutia, N.D. Chkhaidze, and N. Mulders, *Fiz. Nizk. Temp.* **35**, 962 (2009) [*Low Temp. Phys.* **35**, 752 (2009)].
11. A. Falicov and A.N. Berker, *J. Low Temp. Phys.* **107**, 51 (1996).
12. L.D. Landau and E.M. Lifshitz, *Statistical Physics*, Nauka, Moscow (1976), P. 1, p. 309.
13. M. Chester, J.-P. Laheurte, and J.-P. Romagnan, *Phys. Rev.* **B14**, 2812 (1976).
14. E.S. Sabisky and C.H. Andersen, *Phys. Rev.* **A7**, 790 (1973).
15. Yu.P. Monarkha and S.S. Sokolov, *Fiz. Nizk. Temp.* **15**, 339 (1989) [*Low Temp. Phys.* **15**, 191 (1989)].